IJME

Int. J. of Applied Mechanics and Engineering, ????, vol.??, No.?, pp.???-???
DOI: 10.59441/ijame/226467

HYDROELASTIC WAVE PROPAGATION IN A DISPERSED VISCOUS FLUID FLOWING THROUGH A VISCOELASTIC TUBE

R. Tagiyev[1*] and M. Tagiyev[2]
[1]Faculty of information technology and management, Azerbaijan State Oil and Industry University, AZERBAIJAN
[2]Faculty of Mechanics and Mathematics, Baku State University, AZERBAIJAN
E-mail: tagiyev.reshad@asoiu.edu.az

An analytical model is developed for small-amplitude hydroelastic wave propagation in an incompressible dispersed viscous fluid flowing through a thin-walled viscoelastic tube. The dispersed medium is described by an effective-medium approximation with a velocity-equilibrium, or no-slip, assumption between the carrier fluid and dispersed particles. Concentration-dependent viscosity is introduced using Einstein's relation, Taylor's droplet model, and an ellipsoidal-particle correction, while the tube wall is modeled by Rabotnov's linear hereditary theory. The continuity and momentum equations are coupled with the hereditary wall relation to obtain an integro-differential equation for the radial wall displacement. A Fourier spectral representation is used to derive explicit expressions for the wave speed, attenuation coefficient, velocity amplitude, and hydraulic impedance. For $0 \le \varphi \le 0.2$, the wave speed decreases by $1.8 - 2.7\%$ for Taylor's model and by 20.8% for the ellipsoidal-particle model with $K_e = 16.2$. The attenuation coefficient increases by factors of $1.28 - 1.41$ and 3.36, respectively, while the velocity amplitude decreases by $4.2 - 6.3\%$ and 36.7%. The model reduces to the classical homogeneous-fluid and elastic-tube limits, confirming its physical consistency.

Keywords: hydroelastic wave propagation, dispersed viscous fluid, concentration-dependent viscosity, hereditary viscoelasticity, Fourier spectral method.

1. Introduction

Wave propagation in viscous fluids confined within deformable or viscoelastic conduits is an important problem in fluid mechanics, hydroelasticity, and applied mathematics. Such processes occur in pipeline transport, hydraulic systems, oil-production tubing, slurry pipelines, and other multiphase-flow applications. In these systems, the interaction between the internal flow and the compliant wall may significantly influence pressure transients, wave speed, attenuation, and flow stability.

The theoretical basis of hydroelastic wave motion is associated with classical fluid dynamics and fluid-structure interaction theory [1, 2]. When the conduit wall is viscoelastic, its deformation depends not only on the instantaneous pressure but also on the previous deformation history of the wall material. In the present study, this delayed mechanical response is referred to as wall memory and is described using Rabotnov's linear hereditary theory [3].

In many engineering applications, the transported medium cannot be treated as a homogeneous single-phase fluid. It may contain suspended solid particles, liquid droplets, bubbles, or other dispersed inclusions. The averaged behavior of such media can be described within the framework of multiphase-flow theory [4]. For dilute dispersed systems, Einstein's relation gives the classical viscosity correction for rigid spherical particles [5], while Taylor's model describes the effective viscosity of fluids containing small liquid droplets [6]. More general rheological studies show that particle shape, droplet deformation, and viscosity contrast may also affect the effective viscosity of dispersed systems [7-9].

* To whom correspondence should be addressed.

The compliance and rheology of the tube wall play a central role in hydroelastic wave propagation. Classical water-hammer and pipe-transient studies showed that wall deformability changes pressure-wave speed and damping [10-12]. Later investigations demonstrated that viscoelastic pipe-wall behavior may introduce additional attenuation, dispersion, and fluid–structure interaction effects [13-14]. Related studies on bubbly liquids, multiphase pressure transients, hydraulic impedance, and wave dispersion further confirm that the transported medium and the wall response must be considered together in transient-flow analysis [15-18].

Suspension flows through deformable conduits and transient flows in viscoelastic pipelines have been analyzed in related theoretical and numerical studies [19-22]. Analytical and semi-analytical methods are also useful in such problems because they provide explicit relations between physical parameters and wave characteristics. In particular, sweep-based algorithms, hyperbolic-system formulations, and Laplace-transform techniques have been applied to related pipeline, gas-lift, and oil-extraction models [23-25].

General fluid-structure interaction theory and computational multiphase-flow modeling provide additional background for the present formulation [26-28]. Recent studies on transient flow in viscoelastic pipes and granular-slurry pipelines show that wall rheology, energy dissipation, particle diameter, and particle concentration may strongly influence wave evolution and attenuation [29-31]. Hydroelastic waves have also been investigated in free-surface and stratified-fluid configurations, including head-on collision processes of hydroelastic solitary waves and thermocapillary solitary-wave interactions in viscoelastic fluids [32-34].

Despite these developments, the combined analytical treatment of dispersed viscous fluids in viscoelastic tubes remains insufficiently developed. Most existing formulations consider either homogeneous viscous fluids interacting with viscoelastic walls or dispersed media flowing in rigid or weakly deformable conduits. Therefore, the simultaneous influence of concentration-dependent viscosity, particle geometry, hereditary wall memory, and hydraulic impedance on hydroelastic wave attenuation requires further investigation.

The present study develops an analytical model for small-amplitude hydroelastic wave propagation in an incompressible dispersed viscous fluid flowing through a thin-walled viscoelastic tube. The dispersed medium is described by an effective-medium approximation with a velocity-equilibrium, or no-slip, assumption between the carrier fluid and the dispersed phase. The tube wall is modeled using Rabotnov's hereditary theory. The Fourier spectral formulation transforms the integro-differential wave problem into separate harmonic components and makes it possible to obtain explicit expressions for the wave speed, attenuation coefficient, velocity amplitude, and hydraulic impedance.

2. Problem statement

We consider small-amplitude hydroelastic wave propagation in an incompressible dispersed viscous fluid flowing through a thin-walled circular viscoelastic tube. The undeformed tube radius is denoted by R, and the wall thickness is denoted by h. The longitudinal coordinate is x, and time is t. The radial displacement of the tube wall is denoted by $w(x,t)$, while $u(x,t)$ denotes the averaged axial velocity of the dispersed mixture.

The analysis is carried out in dimensional form, and all numerical parameters are expressed in SI units. The dispersed medium is described within an effective-medium approximation for multiphase systems [4]. The carrier fluid and suspended particles are assumed to move with the same averaged velocity; therefore, slip between phases is neglected. The particle volume concentration is denoted by φ. The hydrodynamic pressure is denoted by $p(x,t)$, and the effective dynamic viscosity of the dispersed mixture is denoted by μ. The symbols μ_0 and μ_1 are used for the dynamic viscosities of the carrier fluid and the droplet phase, respectively.

Under the assumptions of one-dimensional axisymmetric motion and small wall deformation, the continuity equation is written as:

$$\frac{\partial u}{\partial x}+\frac{2}{R}\frac{\partial w}{\partial t}=0. \tag{2.1}$$

Equation (2.1) expresses conservation of volume in a deformable tube.

The one-dimensional momentum equation of the dispersed viscous mixture is taken in the form

$$\rho\frac{\partial u}{\partial t}+\frac{\partial p}{\partial x}+\frac{8\mu}{R^2}u=0, \tag{2.2}$$

where ρ is the averaged density of the dispersed mixture. The last term in Eq.(2.2) represents viscous hydraulic resistance.

Differentiating Eq.(2.1) with respect to time and Eq.(2.2) with respect to x, and then eliminating $\partial u/\partial x$, gives:

$$\frac{\partial^2 p}{\partial x^2}-=\frac{2\rho}{R}\frac{\partial^2 w}{\partial t^2}+\frac{16\mu}{R^3}\frac{\partial w}{\partial t}.$$

Thus, the longitudinal curvature of the pressure field is expressed through the radial acceleration and radial velocity of the tube wall.

The pressure acting on the thin viscoelastic tube wall is related to the radial displacement by:

$$p(x,t)=\frac{h}{R^2}E^*w(x,t),$$

where E^* is the hereditary elastic operator of the wall material. According to Rabotnov's linear hereditary theory [3], this operator is defined as:

$$E^v w(x,t)=E\left[w(x,t)-\int_{-\infty}^{t}\Gamma(t-\tau)w(x,\tau)d\tau\right], \tag{2.3}$$

where E is the instantaneous elastic modulus of the wall material and $\Gamma(t-\tau)$ is the relaxation kernel. The integral term represents the wall-memory effect.

Using Eq.(2.3), the pressure becomes:

$$p(x,t)=\frac{Eh}{R^2}\left[w(x,t)-\int_{-\infty}^{t}\Gamma(t-\tau)w(x,\tau)d\tau\right].$$

Since the relaxation kernel depends only on time, differentiating this relation twice with respect to x and substituting it into the pressure-curvature relation above gives:

$$\frac{\partial^2 w(x,t)}{\partial x^2}-\int_{-\infty}^{t}\Gamma(t-\tau)\frac{\partial^2 w(x,\tau)}{\partial x^2}d\tau-\frac{2\rho R}{Eh}\frac{\partial^2 w(x,t)}{\partial t^2}-\frac{16\mu}{REh}\frac{\partial w(x,t)}{\partial t}=0.$$

To introduce the reference hydroelastic wave speed, we consider the purely elastic and non-dissipative limiting case. In this case, the hereditary kernel and viscous term are neglected, and the classical thin-wall hydroelastic wave speed becomes:

$$c_0^2=\frac{Eh}{2\rho R}. \tag{2.4}$$

The dimensional consistency of Eq.(2.4) follows from:

$$\frac{Eh}{\rho R} \sim \frac{Pa \cdot m}{\left(kg/m^3\right)m} = \frac{m^2}{s^2},$$

which confirms that c_0 has the dimension of velocity.

Using Eq.(2.4), the governing integro-differential equation for the radial displacement of the viscoelastic tube wall is obtained as:

$$\frac{\partial^2 w(x,t)}{\partial x^2} - \int_{-\infty}^{t} \Gamma(t-\tau)\frac{\partial^2 w(x,\tau)}{\partial x^2}d\tau - \frac{8\mu}{\rho R^2 c_0^2}\frac{\partial w(x,t)}{\partial t} - \frac{1}{c_0^2}\frac{\partial^2 w(x,t)}{\partial t^2} = 0. \tag{2.5}$$

Equation (2.5) is the governing wave equation of the present model. The hereditary integral accounts for wall memory, the third term describes viscous dissipation in the dispersed mixture, and the last term represents fluid inertia. In the limiting case of a purely elastic wall and a homogeneous viscous fluid, Eq.(2.5) reduces to the classical hydroelastic wave formulation.

3. Fourier spectral representation of the solution

To solve Eq.(2.5), we use a Fourier spectral representation in time. This approach is suitable for periodic pressure disturbances and allows the hereditary integro-differential problem to be reduced to separate harmonic equations. The radial displacement is represented as

$$w(x,t) = \sum_{s=1}^{N} y_s(x)\exp(is\omega t), \tag{3.1}$$

where s is the harmonic index, N is the number of retained harmonic components, $y_s(x)$ is the spatial amplitude of the s -th harmonic, and ω is the prescribed angular frequency.

Substitution of Eq.(3.1) into the hereditary integral in Eq.(2.5) gives

$$\int_{-\infty}^{t} \Gamma\left(t-\tau\right)\frac{\partial^2 w\left(x,\tau\right)}{\partial x^2}d\tau = \int_{-\infty}^{t} \Gamma\left(t-\tau\right)\sum_{s=1}^{N} y_s''\left(x\right)\exp\left(is\omega\tau\right)d\tau.$$

Since $y_s(x)$ depends only on the spatial coordinate, $y_s''(x)$ can be taken outside the time integral. Introducing $\theta = t-\tau,\ \tau = t-\theta,$ we obtain:

$$\int_{-\infty}^{t} \Gamma\left(t-\tau\right)y_s''\left(x\right)\exp\left(is\omega t\right)d\tau = y_s''\left(x\right)\exp\left(is\omega t\right)\int_{0}^{\infty} \Gamma\left(\theta\right)\exp\left(-is\omega\theta\right)d\theta.$$

Thus, the frequency-domain hereditary coefficient is defined as:

$$\alpha_s = \int_{0}^{\infty} \Gamma\left(\theta\right)\exp\left(-is\omega t\right)d\theta. \tag{3.2}$$

This transformation follows the standard frequency-domain treatment of linear hereditary operators [3]. The coefficient α_s characterizes the contribution of the relaxation kernel at the harmonic frequency $s\omega$. In general, α_s is complex and therefore affects both the elastic and dissipative parts of the wall response.

Using Eq.(3.2), the hereditary term becomes

$$\sum_{s=1}^{N} \alpha_s y_s''(x) \exp(is\omega t).$$

Substituting Eq.(3.1) into Eq.(2.5), using the expression above for the hereditary term, and collecting the coefficients of $\exp(is\omega t)$, we obtain:

$$(1-\alpha_s) y_s''(x) + \left[\frac{s^2\omega^2}{c_0^2} - i\frac{\delta s\omega\mu}{\rho R^2 c_0^2} \right] y_s(x) = 0.$$

Dividing this equation by $1-\alpha_s$, we write:

$$y_s''(x) + \delta_s^2 y_s(x) = 0, \tag{3.3}$$

where: $$\delta_s^2 = \frac{\frac{s^2\omega^2}{c_0^2} - i\frac{\delta s\omega\mu}{\rho R^2 c_0^2}}{1-\alpha_s} = \frac{s\omega}{c_0^2}\left(s\omega - i\frac{\delta\mu}{\rho R^2} \right)(1-\alpha_s)^{-1}.$$

Here, δ_s is the complex propagation parameter of the s-th harmonic. The notation separates the harmonic index s, the number of retained harmonics N, and the propagation parameter δ_s.

For the subsequent analysis of wave attenuation caused by the dispersed medium, we consider the fundamental harmonic in the absence of hereditary correction: $s=1,\ \alpha_1 = 0.$

Then Eq.(3.3) reduces to

$$y^n(x) + \delta^2 y(x) = 0, \tag{3.4}$$

where: $$\delta^2 = \frac{\omega}{c_0^2}\left(\omega - i\frac{\delta\mu}{\rho R^2} \right).$$

The complex quantity δ^2 can be written as:

$$\delta^2 = \lambda_0 - i\lambda_1,$$

where: $$\lambda_0 = \frac{\omega^2}{c_0^2},\ \lambda_1 = \frac{\delta\omega\mu}{\rho R^2 c_0^2}.$$

For wave propagation in the positive x-direction, the spatial dependence is taken in the form $\exp(-i\delta x)$. To obtain a physically admissible damped wave, the complex propagation parameter is selected as:

$$\delta = \delta_0 - i\delta_1, \qquad \delta_0 > 0, \qquad \delta_1 > 0. \tag{3.5}$$

Indeed:

$$\exp(-i\delta x) = \exp\left[-i(\delta_0 - i\delta_1)x\right] = \exp(-i\delta_0 x)\cdot\exp(-\delta_1 x).$$

Thus:

$$\mathrm{Im}(\delta) < 0,$$

ensures exponential attenuation along the positive x-direction.

The real and imaginary parts of δ are given by:

$$\delta_0 = \left\{\frac{1}{2}(m+\lambda_0)\right\}^{\frac{1}{2}}, \quad \delta_1 = \left\{\frac{1}{2}(m-\lambda_0)\right\}^{\frac{1}{2}},$$

where: $m = \sqrt{\lambda_0^2 + \lambda_1^2}$.

Here, δ_0 determines the phase variation of the wave, while δ_1 is the attenuation coefficient. The phase wave speed is therefore:

$$c = \frac{\omega}{\delta_0}. \tag{3.6}$$

The general solution of Eq.(3.4) is $y(x) = A\exp(-i\delta x) + B\exp(i\delta x)$, where A and B are constants corresponding to waves propagating in opposite directions. Hence, the radial wall displacement is:

$$w(x,t) = \left[A\exp(-i\delta x) + B\exp(i\delta x)\right]\cdot\exp(i\omega t).$$

Using the thin-wall relation between pressure and radial displacement, the pressure field becomes:

$$p(x,t) = \frac{Eh}{R^2}\left[A\exp(-i\delta x) + B\exp(i\delta x)\right]\exp(i\omega t). \tag{3.7}$$

The averaged axial velocity is obtained from the momentum equation. For the harmonic representation:

$$u(x,t) = U(x)\exp(i\omega t).$$

Eq.(2.2) gives:

$$\left(i\omega\rho + \frac{8\mu}{R^2}\right)U(x) + \frac{dp}{dx} = 0.$$

Introducing the hydraulic impedance in this form is consistent with the standard pressure-gradient/velocity representation used in one-dimensional transient-flow analysis [18]. We define:

$$J = i\omega\rho + \frac{8\mu}{R^2}.$$

Then:

$$\frac{dp}{dx} = -JU(x).$$

Substituting Eq.(3.7) into this relation yields:

$$u(x,t) = \frac{i\delta hE}{R^2 J}\left[A\exp(-i\delta x) - B\exp(i\delta x)\right]\cdot\exp(i\omega t).$$

The hydraulic impedance J contains two physical contributions. Its real part:

$$\mathrm{Re}(J) = \frac{8\mu}{R^2},$$

represents viscous hydraulic resistance, while its imaginary part:

$$\mathrm{Im}(J) = \omega\rho,$$

represents the inertial contribution of the unsteady flow. Therefore, the velocity amplitude is affected by both viscous dissipation and fluid inertia.

4. Pipe flow and displacement

We now consider the pressure distribution, radial wall displacement, and averaged axial velocity in a straight viscoelastic tube of finite length l. The coordinate $x = 0$ corresponds to the inlet, while $x = l$ corresponds to the outlet. The harmonic boundary-value formulation used here is consistent with the one-dimensional transient-flow interpretation of hydroelastic waves in deformable conduits [10, 11, 12, 22].

For the fundamental harmonic, the pressure field obtained in Eq.(3.7) has the form:

$$p(x,t) = \frac{Eh}{R^2}\left[A\exp(-i\delta x) + B\exp(i\delta x)\right]\cdot\exp(i\omega t).$$

The constants A and B are determined from the boundary conditions. The inlet pressure is prescribed harmonically, and the pressure disturbance at the outlet is assumed to vanish. Therefore, we impose:

$$p(0,t) = p_0\exp(i\omega t), \quad p(l,t) = 0. \tag{4.1}$$

Here, p_0 is the prescribed inlet pressure amplitude. Substitution of the pressure representation into Eq.(4.1) gives the algebraic system:

$$A + B = p_0 \frac{R^2}{Eh},$$

$$A\exp\left(-i\delta l\right) + B\exp\left(i\delta l\right) = 0.$$

Solving this system, we obtain:

$$A = \frac{p_0 R^2}{Eh}\frac{\exp\left(i\delta l\right)}{\exp\left(i\delta l\right) - \exp\left(-i\delta l\right)}, \qquad B = -\frac{p_0 R^2}{Eh}\frac{\exp\left(-i\delta l\right)}{\exp\left(i\delta l\right) - \exp\left(-i\delta l\right)}.$$

Substituting these constants into the pressure expression yields:

$$p\left(x,t\right) = p_0 \frac{\sin\left(\delta\left(l-x\right)\right)}{\sin\left(\delta l\right)}\exp\left(i\omega t\right).$$

Using the thin-wall relation between pressure and radial displacement, the wall displacement is obtained as:

$$w\left(x,t\right) = \frac{R^2 p_0}{Eh}\frac{\sin\left(\delta\left(l-x\right)\right)}{\sin\left(\delta l\right)}\exp\left(i\omega t\right).$$

The averaged axial velocity follows from the impedance relation derived in Section 3, $\frac{dp}{dx} = -Ju.$ Differentiating the pressure expression with respect to x and using this relation gives:

$$u\left(x,t\right) = \frac{\delta p_0}{J}\frac{\cos\left(\delta\left(l-x\right)\right)}{\sin\left(\delta l\right)}\exp\left(i\omega t\right).$$

Thus, the finite-length tube solution can be written as:

$$p\left(x,t\right) = p_0 \frac{\sin\left(\delta\left(l-x\right)\right)}{\sin\left(\delta l\right)}\exp\left(i\omega t\right),$$

$$w\left(x,t\right) = \frac{R^2 p_0}{Eh}\frac{\sin\left(\delta\left(l-x\right)\right)}{\sin\left(\delta l\right)}\exp\left(i\omega t\right), \tag{4.2}$$

$$u\left(x,t\right) = \frac{\delta p_0}{J}\frac{\cos\left(\delta\left(l-x\right)\right)}{\sin\left(\delta l\right)}\exp\left(i\omega t\right).$$

Equation (4.2) satisfies the prescribed inlet pressure condition and the zero outlet pressure disturbance condition given in Eq.(4.1).

To obtain the limiting case of a semi-infinite tube, we consider the limit $l \to \infty$. The complex propagation parameter was selected in Section 3 as $\delta = \delta_0 - i\delta_1,\ \delta_1 > 0.$

Therefore, $\mathrm{Im}(\delta) < 0$. This condition is essential for spatial attenuation in the positive x-direction. Indeed:

$$\exp(-i\delta x) = \exp\left(-i(\delta_0 - i\delta_1)x\right) = \exp(-i\delta_0 x)\exp(-\delta_1 x).$$

Thus, the factor $\exp(-\delta_1 x)$ describes exponential decay of the wave amplitude.

For $l \to \infty$ and $\mathrm{Im}(\delta) < 0$, the following asymptotic relations hold:

$$\lim_{l\to\infty} \frac{\sin\left(\delta(l-x)\right)}{\sin(\delta l)} = \exp(-i\delta x), \qquad \lim_{l\to\infty} \frac{\cos\left(\delta(l-x)\right)}{\sin(\delta l)} = i\cdot\exp(-i\delta x).$$

Substitution of these limits into Eq.(4.2) gives the semi-infinite tube solution:

$$p(x,t) = p_0 \exp\left(i(\omega t - \delta x)\right),$$

$$w(x,t) = \frac{R^2 p_0}{Eh}\exp\left(i(\omega t - \delta x)\right), \tag{4.3}$$

$$u(x,t) = \frac{i\delta p_0}{J}\exp\left(i(\omega t - \delta x)\right).$$

Since:

$$\delta = \delta_0 - i\delta_1,$$

the common exponential factor in Eq.(4.3) can be written as:

$$\exp\left(i(\omega t - \delta x)\right) = \exp\left(i(\omega t - \delta_0 x)\right)\exp(-\delta_1 x).$$

Therefore, the observable amplitudes of pressure, radial displacement, and averaged axial velocity decay exponentially along the tube. Taking the modulus of Eq.(4.3), we obtain:

$$|p(x)| = |p_0|\exp(-\delta_1 x),$$

$$|w(x)| = \frac{R^2|p_0|}{Eh}\exp(-\delta_1 x), \tag{4.4}$$

$$|u(x)| = \frac{|\delta||p_0|}{|J|}\exp(-\delta_1 x),$$

Here:

$$|\delta| = \sqrt{\delta_0^2 + \delta_1^2}, \quad |J| = \sqrt{\left(\frac{8\mu}{R^2}\right)^2 + (\omega\rho)^2}.$$

Equation (4.4) shows that the attenuation coefficient δ_1 controls the spatial decay of pressure, wall displacement, and velocity amplitudes. The velocity amplitude is additionally affected by the hydraulic impedance J, which contains both viscous resistance and fluid inertia.

5. Viscosity correction and numerical evaluation

We now introduce the concentration-dependent viscosity corrections used to evaluate the influence of the dispersed phase on the wave speed, attenuation coefficient, and velocity amplitude. Since the effective viscosity μ enters the complex propagation parameter and the hydraulic impedance, changes in μ directly affect both wave attenuation and flow resistance.

The numerical evaluation focuses mainly on the influence of concentration-dependent viscosity on wave speed, attenuation, and velocity amplitude. The hereditary wall contribution is retained in the analytical formulation through the frequency-domain coefficient αs, while a separate parametric study of the relaxation kernel may be considered in future work.

The viscosity models considered below are used under the assumption of a dilute or moderately dilute dispersed system. In this approximation, particle-particle hydrodynamic interactions, aggregation, sedimentation, and non-Newtonian effects of the carrier phase are neglected. Therefore, the results obtained near the upper concentration limit should be interpreted as qualitative analytical trends rather than exact quantitative predictions.

For rigid spherical particles, the classical Einstein correction is used [5]:

$$\mu = \mu_0 \left(1 + 2.5\varphi\right), \tag{5.1}$$

where μ_0 is the dynamic viscosity of the carrier fluid. Equation (5.1) is strictly valid for dilute suspensions. In the present study, the interval $0 \le \varphi \le 0.2$ is used as a comparative analytical range for studying the relative influence of different viscosity models.

To account for the effect of particle shape, an ellipsoidal-particle correction is also considered. Non-spherical rigid inclusions generally produce stronger resistance to the carrier flow than spherical particles. This effect is represented in the simplified form:

$$\mu = \mu_0 \left(1 + K_e\varphi\right), \tag{5.2}$$

where K_e is the shape coefficient. In the numerical calculations, $K_e = 16.2$ is used as a representative high-resistance non-spherical case. This model is included to compare the influence of particle geometry on hydroelastic wave attenuation. The use of shape-dependent viscosity corrections is consistent with rheological descriptions of dispersed systems with non-spherical inclusions [7-9].

For liquid droplets, Taylor's viscosity model is used [6]:

$$\mu = \mu_0 \left[1 + 2.5\varphi \left(\frac{\mu_1 + \frac{2}{5}\mu_0}{\mu_1 + \mu_0} \right) \right], \tag{5.3}$$

where μ_1 is the dynamic viscosity of the droplet phase. Taylor's model represents deformable liquid inclusions, while Eq.(5.2) represents non-spherical rigid particles. Thus, Eqs.(5.1)–(5.3) allow the comparison of different dispersed-phase geometries: rigid spherical particles, rigid ellipsoidal particles, and liquid droplets.

In the limiting case $\mu_1 \to \infty$, the liquid droplet behaves as a rigid inclusion, and Taylor's formula approaches Einstein's correction.

For the numerical evaluation, the analysis is carried out in dimensional form. All parameter values are written in SI units:

$$R = 0.005\,m, \quad h = 0.1R = 5 \cdot 10^{-4}\,m, \quad \mu_0 = 0.01\,Pa \cdot s, \quad E = 4 \cdot 10^5\,Pa,$$

$$\rho = 1000\,kg/m^3, \quad \omega = 2\pi s^{-1}, \quad x = 0.1\,m, \quad p_0 = 100\,Pa.$$

For Taylor's model, the viscosity ratios:

$$\mu_1 / \mu_0 = 0.5,\ 1,\ 5$$

are considered. The wave speed is calculated from Eq.(3.6), while the attenuation coefficient and velocity amplitude are evaluated using Eqs.(3.5), (4.4), and the viscosity corrections (5.1)-(5.3).

The percentage decrease in wave speed is calculated relative to the value at zero concentration:

$$\Delta c(\%) = \frac{c(0) - c(\varphi_{\max})}{c(0)} \cdot 100, \quad \varphi_{\max} = 0.2. \tag{5.4}$$

Similarly, the decrease in velocity amplitude is evaluated as:

$$\Delta |u|(\%) = \frac{|u(0)| - |u(\varphi_{\max})|}{|u(0)|} \cdot 100. \tag{5.5}$$

The relative increase in attenuation is measured by:

$$I_{\delta_1} = \frac{\delta_1(\varphi_{\max})}{\delta_1(0)}. \tag{5.6}$$

Equations (5.4)-(5.6) define the reference values and concentration interval used for the percentage estimates. This avoids ambiguity in the interpretation of the numerical changes.

The numerical results show that increasing the particle volume concentration φ increases the effective viscosity of the dispersed mixture. As a result, the real part of the hydraulic impedance:

$$\mathrm{Re}(J) = \frac{8\mu}{R^2},$$

also increases. This produces stronger viscous resistance and reduces the velocity amplitude. At the same time, the dissipative part of the complex propagation parameter increases, which leads to a larger attenuation coefficient δ_1.

For $0 \le \varphi \le 0.2$, the wave speed decreases by approximately $1.8 - 2.7\%$ for Taylor's droplet model, depending on the viscosity ratio μ_1 / μ_0. For the ellipsoidal-particle model with $K = 16.2$, the corresponding decrease is approximately 20.8%. Over the same concentration range, the attenuation coefficient increases by a factor of approximately $1.28 - 1.41$ for Taylor's model and by about 3.36 for the ellipsoidal-particle model.

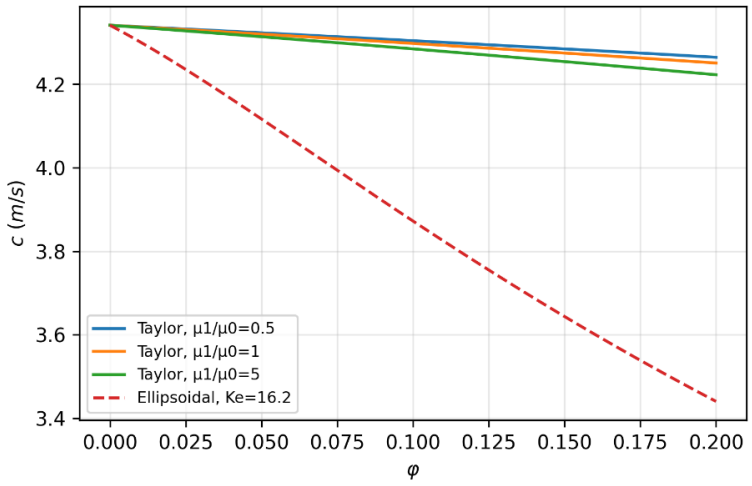

Fig.1. Wave propagation speed versus particle volume concentration.

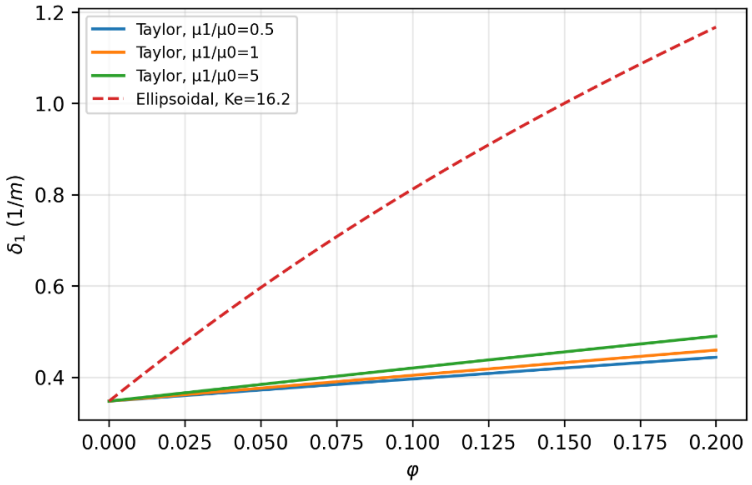

Fig.2. Attenuation coefficient versus particle volume concentration.

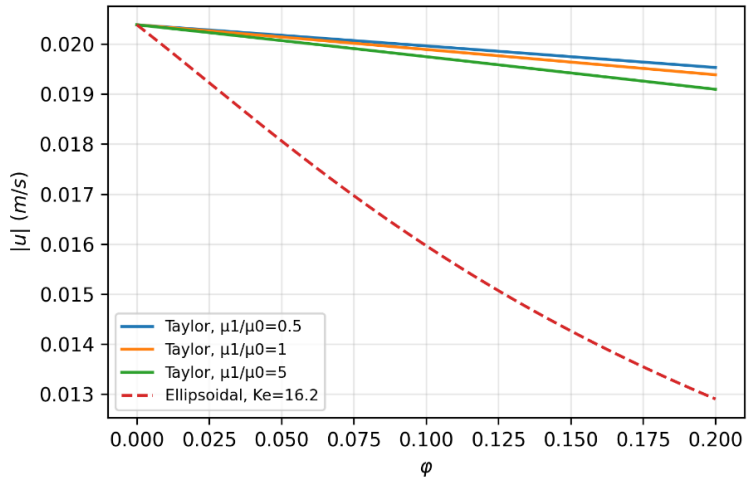

Fig.3. Flow velocity amplitude versus particle volume concentration.

The velocity amplitude decreases by approximately $4.2-6.3\%$ for Taylor's model and by about 36.7% for the ellipsoidal-particle model.

These results indicate that particle geometry has a substantial influence on hydroelastic wave damping. The ellipsoidal-particle model produces a larger effective viscosity than Taylor's droplet model. Therefore, it yields stronger attenuation and a larger reduction in velocity amplitude.

Figures 1-3 illustrate the dependence of the wave speed, attenuation coefficient, and velocity amplitude on the particle volume concentration.

6. Validation and limiting cases

The validity of the proposed analytical formulation is examined through limiting-case analysis and comparison with classical hydroelastic wave models. Since the present model extends the standard one-dimensional wave formulation by including concentration-dependent viscosity and hereditary wall memory, its consistency must be verified when these additional effects are removed.

First, we consider the limiting case in which the dispersed phase is absent. This corresponds to $\varphi = 0$. In this case, the effective viscosity of the mixture reduces to the viscosity of the carrier fluid, $\mu = \mu_0$.

Therefore, the governing equation (2.5) describes wave propagation in a homogeneous viscous fluid flowing through a viscoelastic tube. This limiting behavior is consistent with classical transient-flow models in deformable and viscoelastic pipes [10-13, 29-30].

Second, the purely elastic-wall limit is obtained by neglecting the hereditary memory term. In this case, $\Gamma(t-\tau) = 0,\ \alpha_s = 0$.

Then the wall response becomes instantaneous, and the hereditary wall relation reduces to the classical elastic thin-wall relation $p(x,t) = \dfrac{Eh}{R^2} w(x,t)$.

Under the additional assumption of negligible viscous dissipation, the model yields the reference hydroelastic wave speed $c_0^2 = \dfrac{Eh}{2\rho R}$, which coincides with the standard wave-speed expression for hydroelastic wave propagation in an elastic tube [10-12].

Third, if both dispersed-phase effects and hereditary wall memory are neglected, the model reduces to the classical one-dimensional hydroelastic wave formulation for a homogeneous fluid in an elastic tube. In this limit, the wave behavior is governed only by fluid inertia and wall elasticity. Thus, the additional terms introduced in the present model do not alter the known classical limit, but extend it by incorporating viscous dissipation, concentration-dependent rheology, and wall memory.

The attenuation behavior also has the correct physical form. In Section 3, the complex propagation parameter was selected as $\delta = \delta_0 - i\delta_1,\ \delta_1 > 0$.

Therefore, the wave factor can be written as:

$$\exp\left(i\left(\omega t - \delta x\right)\right) = \exp\left(i\left(\omega t - \delta_0 x\right)\right)\exp\left(-\delta_1 x\right).$$

This expression shows that the wave amplitude decreases exponentially in the positive x-direction. Hence, the selected branch of the complex propagation parameter corresponds to a physically admissible damped wave.

The semi-infinite tube solution obtained in Eq.(4.3) and the amplitude expressions in Eq.(4.4) are also consistent with this attenuation mechanism. In particular, pressure, wall displacement, and velocity amplitudes all contain the common decay factor $\exp\left(-\delta_1 x\right)$.

This confirms that the attenuation coefficient δ_1 has a direct physical interpretation as the spatial damping rate of the hydroelastic wave.

Therefore, the proposed formulation reproduces the expected limiting cases of hydroelastic wave propagation in homogeneous fluids and elastic or viscoelastic tubes. At the same time, it extends the classical framework by including particle-concentration effects, particle-geometry-dependent viscosity, hereditary wall response, and hydraulic impedance.

7. Conclusion

In this study, an analytical model was developed for small-amplitude hydroelastic wave propagation in an incompressible dispersed viscous fluid flowing through a thin-walled viscoelastic tube. The main contribution of the work is the simultaneous consideration of concentration-dependent effective viscosity of the dispersed medium and hereditary wall-memory effects of the viscoelastic tube.

The governing integro-differential equation was derived by coupling the continuity and momentum equations of the dispersed viscous mixture with the hereditary wall relation. A Fourier spectral representation was used to reduce the wave problem to harmonic components and to obtain explicit expressions for the wave speed, attenuation coefficient, velocity amplitude, and hydraulic impedance.

The results show that increasing the particle volume concentration increases the effective viscosity of the dispersed mixture. This strengthens viscous resistance, reduces the velocity amplitude, and increases the attenuation coefficient. For $0 \le \varphi \le 0.2$, the wave speed decreases by approximately $1.8 - 2.7\%$ for Taylor's droplet model, depending on the viscosity ratio μ_1 / μ_0. For the ellipsoidal-particle model with $K_e = 16.2$, the corresponding decrease is approximately 20.8%. Over the same concentration range, the attenuation coefficient increases by a factor of approximately $1.28 - 1.41$ for Taylor's model and by about 3.36 for the ellipsoidal-particle model. The velocity amplitude decreases by approximately $4.2 - 6.3\%$ for Taylor's model and by about 36.7% for the ellipsoidal-particle model.

These findings indicate that particle geometry has a significant influence on hydroelastic wave damping. Non-spherical particles produce a larger increase in effective viscosity than deformable liquid droplets. As a result, they lead to stronger attenuation and a larger reduction in flow velocity amplitude.

The limiting-case analysis confirms the physical consistency of the formulation. In the absence of dispersed particles, the model reduces to the homogeneous viscous-fluid case. When hereditary wall memory is neglected, the formulation approaches the classical elastic-tube hydroelastic wave model. The selected complex propagation branch also provides a physically admissible spatial attenuation of the wave amplitude.

The present model has several limitations. The analysis is restricted to small-amplitude waves, one-dimensional axisymmetric flow, dilute or moderately dilute dispersed systems, Newtonian effective viscosity, and linear hereditary wall response. Particle-particle interactions, nonlinear wave effects, non-Newtonian carrier-fluid behavior, and possible slip between phases are not considered.

Future extensions may include nonlinear wave regimes, polydisperse particle distributions, non-Newtonian carrier fluids, more general hereditary kernels, and comparison with experimental or high-fidelity numerical data. Such developments would extend the applicability of the present analytical framework to a wider range of deformable multiphase-flow systems, including slurry pipelines and wellbore transport processes.

Nomenclature

A, B – integration constants corresponding to waves propagating in opposite directions
c – phase wave speed
c_0 – reference hydroelastic wave speed
E – instantaneous elastic modulus of the tube wall material
$E*$ – hereditary elastic operator
h – thickness of the tube wall
I_{δ_1} – relative increase in the attenuation coefficient
i – imaginary unit
J – hydraulic impedance

K_e – shape coefficient for ellipsoidal particles
l – length of the tube
m – auxiliary modulus parameter in the complex-root representation
N – number of retained harmonic components
$p(x,t)$ – hydrodynamic pressure
p_0 – prescribed inlet pressure amplitude
R – undeformed radius of the tube
s – harmonic index
$U(x)$ – spatial amplitude of the harmonic velocity field
$u(x,t)$ – averaged axial velocity of the dispersed mixture
$w(x,t)$ – radial displacement of the tube wall
$y_s(x)$ – spatial amplitude of the s -th harmonic component
α_s – frequency-domain hereditary coefficient of the s -th harmonic
$\Gamma(t-\tau)$ – hereditary relaxation kernel
δ – complex propagation parameter of the fundamental harmonic
δ_0 – real part of the complex propagation parameter
δ_1 – attenuation coefficient
δ_s – complex propagation parameter of the s -th harmonic
Δc – percentage decrease in wave speed
$\Delta|u|$ – percentage decrease in velocity amplitude
λ_0, λ_1 – auxiliary parameters used in the complex-root representation
μ – effective dynamic viscosity of the dispersed mixture
μ_0 – dynamic viscosity of the carrier fluid
μ_1 – dynamic viscosity of the droplet phase
ρ – averaged density of the dispersed mixture
τ – time integration variable
φ – particle volume concentration
ω – prescribed angular frequency
θ – auxiliary time variable used in the convolution transformation

References

[1] Loytsyanskiy L.G. (1966): *Mechanics of Liquids and Gases*.– Oxford: Pergamon Press.
[2] Batchelor G.K. (1967): *An Introduction to Fluid Dynamics*.– Cambridge: Cambridge University Press.
[3] Rabotnov Y.N. (1969): *Creep Problems in Structural Members*.– Amsterdam: North-Holland Publishing Company.
[4] Soo S.L. (1967): *Fluid Dynamics of Multiphase Systems*.– Waltham: Blaisdell Publishing Company.
[5] Einstein A. (1906): *Eine neue Bestimmung der Moleküldimensionen*.– Annalen der Physik, vol.324, No.2, pp.289-306.
[6] Taylor G.I. (1932): *The viscosity of a fluid containing small drops of another fluid*.– Proceedings of the Royal Society of London A, vol.138, No.834, pp.41-48.
[7] Pal R. (2016): *Fundamental rheology of disperse systems based on single-particle mechanics*.– Fluids, vol.1, No.4, art.40, https://doi.org/10.3390/fluids1040040.
[8] Maffettone P.L. and Minale M. (1998): *Equation of change for ellipsoidal drops in viscous flow*.– Journal of Non-Newtonian Fluid Mechanics, vol.78, No.2-3, pp.227-241.
[9] Mill C.C. (ed.) (1959): *Rheology of Disperse Systems*.– London: Pergamon Press.
[10] Ghidaoui M.S., Zhao M., McInnis D.A. and Axworthy D.H. (2005): *A review of water hammer theory and practice*.– Applied Mechanics Reviews, vol.58, No.1, pp.49-76, https://doi.org/10.1115/1.1828050.
[11] Wylie E.B., Streeter V.L. and Suo L. (1993): *Fluid Transients in Systems*.– Englewood Cliffs: Prentice Hall.
[12] Tijsseling A.S. (1996): *Fluid-structure interaction in liquid-filled pipe systems: a review*.– Journal of Fluids and Structures, vol.10, No.2, pp.109-146.
[13] Keramat A. and Tijsseling A.S. (2014): *Fluid-structure interaction with viscoelastic pipe-wall behavior*.– Journal of Sound and Vibration, vol.333, pp.466-483.

[14] Wang Y., Li X. and Zhang H. (2019): *Wave attenuation in viscous fluid-filled pipes with viscoelastic walls*.– Applied Mathematical Modelling, vol.67, pp.1-17, https://doi.org/10.1016/j.apm.2018.10.012.
[15] Li Y., Zhang H. and Wang X. (2021): *Wave propagation in viscoelastic pipes conveying bubbly liquids*.– Journal of Fluids and Structures, vol.104, art.103312, https://doi.org/10.1016/j.jfluidstructs.2021.103312.
[16] Yang J., Liu P. and Zhao R. (2022): *Effects of multiphase flow on pressure transients in viscoelastic pipelines*.– International Journal of Multiphase Flow, vol.148, art.103948, https://doi.org/10.1016/j.ijmultiphaseflow.2021.103948.
[17] Zhang C. and Wu Y. (2023): *Attenuation and dispersion of pressure waves in viscoelastic fluid-conveying pipes*.– Applied Mathematical Modelling, vol.118, pp.95-112, https://doi.org/10.1016/j.apm.2023.01.031.
[18] Zhao J., Li B. and Chen X. (2021): *Hydraulic impedance and wave characteristics in viscoelastic pipelines*.– Mechanical Systems and Signal Processing, vol.149, art.107246, https://doi.org/10.1016/j.ymssp.2020.107246.
[19] Misra J.C. and Adhikary S.D. (2016): *Flow of a suspension through deformable conduits*.– Applied Mathematics and Mechanics, vol.37, No.8, pp.1085-1100, https://doi.org/10.1007/s10483-016-2107-9.
[20] Ferrás L.L., Nóbrega J.M. and Pinho F.T. (2019): *Analytical solutions for transient flows in viscoelastic conduits*.– Journal of Non-Newtonian Fluid Mechanics, vol.266, pp.28-37, https://doi.org/10.1016/j.jnnfm.2019.02.004.
[21] Duan H., Ghidaoui M.S., Lee P.J. and Tung Y.K. (2010): *Linear and nonlinear analysis of hydraulic transients in viscoelastic pipes*.– Journal of Fluids and Structures, vol.26, No.5, pp.793-811, https://doi.org/10.1016/j.jfluidstructs.2010.04.006.
[22] Sanada K., Wiggert D.C. and Hatfield F.J. (1990): *Transient analysis of viscoelastic pipelines*.– Journal of Hydraulic Engineering, vol.116, No.11, pp.1325-1340.
[23] Aliev F.A., Aliev N.A., Safarova N.A., Tagiyev R.M. and Rajabov M.F. (2017): *Sweep method for solving the Roesser-type equation describing pipeline motion*.– Applied Mathematics and Computation, vol.295, pp.16-23, https://doi.org/10.1016/j.amc.2016.09.043.
[24] Aliyev N.A., Tagiyev R.M. and Namazov O.Z. (2022): *Algorithm for determining sweep coefficients for solving a second-order hyperbolic system*.– Transactions of the Institute of Mathematics, vol.42, No.1, pp.42-46.
[25] Aliev F.A., Tagiyev R.M., Namazov O.Z. and Turarov A.K. (2025): *Transformation of motion equations in the oil extraction process into Roesser-type equations and their solution using the Laplace transform*.– Computational Methods for Differential Equations, vol.13, No.4, pp.1085-1094.
[26] Païdoussis M.P., Price S.J. and de Langre E. (2011): *Fluid-Structure Interactions: Cross-Flow-Induced Instabilities*.– Cambridge: Cambridge University Press, https://doi.org/10.1017/CBO9780511760792.
[27] Prosperetti A. and Tryggvason G. (eds.) (2009): *Computational Methods for Multiphase Flow*.– Cambridge: Cambridge University Press, https://doi.org/10.1017/CBO9780511609701.
[28] Colombo M. and Fairweather M. (2015): *Multiphase flow modeling in complex pipeline systems*.– International Journal of Multiphase Flow, vol.75, pp.83-99, https://doi.org/10.1016/j.ijmultiphaseflow.2015.05.008.
[29] Tjuatja V., Keramat A., Pan B., Duan H.F., Brunone B. and Meniconi S. (2023): *Transient flow modeling in viscoelastic pipes: a comprehensive review of literature and analysis*.– Physics of Fluids, vol.35, No.8, art.081302, https://doi.org/10.1063/5.0163959.
[30] Xu Y., Zhang Y., Wang X. and Li J. (2024): *Dynamic behavior and mechanism of transient fluid-structure interaction in viscoelastic pipes based on energy analysis*.– Water, vol.16, No.11, art.1468, https://doi.org/10.3390/w16111468.
[31] de Hoog E., van der Ven O., Helmons R., Talmon A. and van Rhee C. (2024): *Experimental research on self-amplifying density waves in horizontal pipelines of two-phase granular slurries: measurements on the effect of particle diameter and concentration*.– International Journal of Multiphase Flow, vol.181, art.105027, https://doi.org/10.1016/j.ijmultiphaseflow.2024.105027.
[32] Bhatti M.M. and Lu D.Q. (2019): *An application of Nwogu's Boussinesq model to analyze the head-on collision process between hydroelastic solitary waves*.– Open Physics, vol.17, No.1, pp.177-191, https://doi.org/10.1515/phys-2019-0018.
[33] Bhatti M.M. and Lu D.Q. (2019): *Hydroelastic solitary wave during the head-on collision process in a stratified fluid*.– Proceedings of the Institution of Mechanical Engineers, Part C: Journal of Mechanical Engineering Science, vol.233, No.17, pp.6135-6148, https://doi.org/10.1177/0954406219840673.
[34] Tariq N., Zhang L., Bhatti M.M., Anwar Bég O. and Oztop H.F. (2026): *Head-on collision between solitary waves and thermocapillary instabilities in Maxwell fluid using Rayleigh-Bénard-Marangoni system*.– International Journal of Numerical Methods for Heat and Fluid Flow, vol.36, No.5, pp.2226-2245, https://doi.org/10.1108/HFF-07-2025-0554.

Received: September 11, 2025
Revised: June 22, 2026